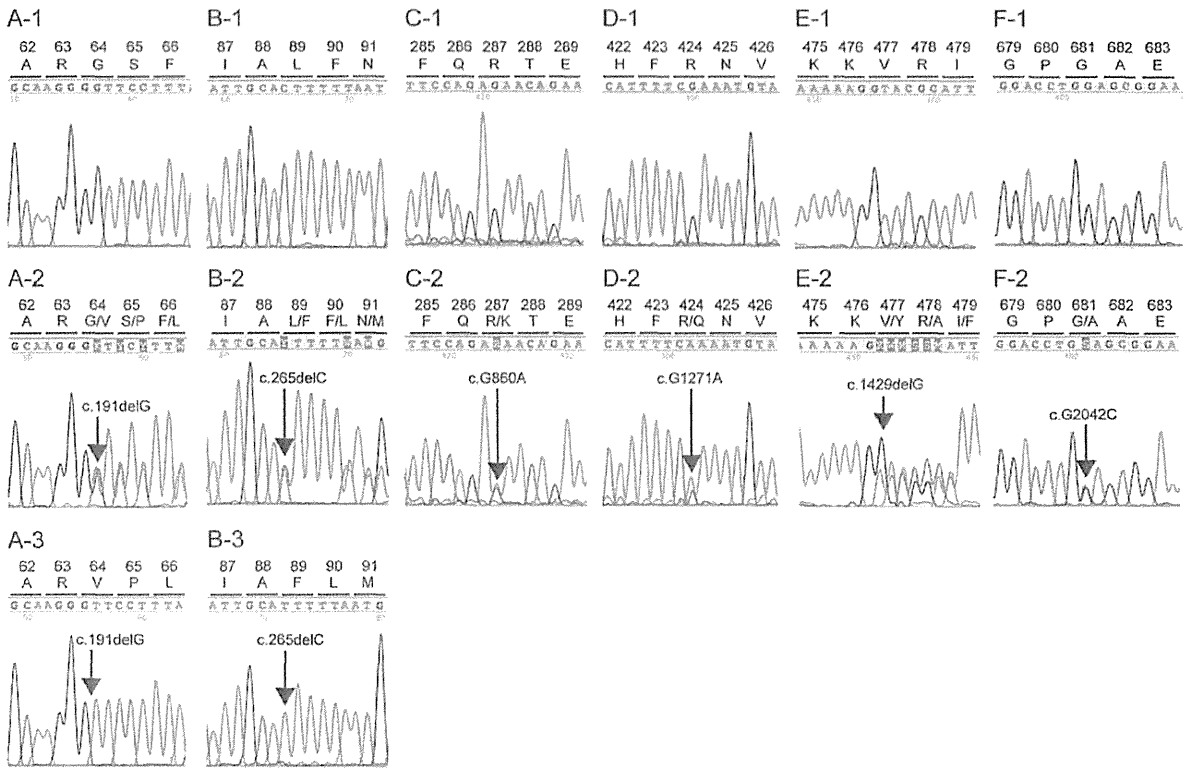

Figure 2. Sequence data of all six identified *CNGA1* mutations in this study. A-1 to F-1 show the normal sequence data for the *CNGA1* gene. A-2 to F-2 show the sequence data for heterozygous *CNGA1* mutations (c.191delG, c.265delC, c.G860A, c.G1271A, c.1429delG and c.G2042C, respectively). A-3 and B-3 show the sequence data for homozygous *CNGA1* mutations (c.191delG and c.265delC).
doi:10.1371/journal.pone.0108721.g002

School of Medicine and Kinki University Faculty of Medicine). The protocol adhered to the tenets of the Declaration of Helsinki, and signed informed consent was obtained from all participants.

Clinical studies

In total, 99 unrelated arRP/spRP patients with no apparent syndrome were recruited from the National Hospital Organization Tokyo Medical Center, Jikei University School of Medicine, Mie University School of Medicine, Nagoya University Graduate School of Medicine, Teikyo University School of Medicine and Kinki University Faculty of Medicine. The patient history was taken and ophthalmic examinations were performed. Clinical diagnosis and evaluation for RP were based on the decimal best-corrected visual acuity (BCVA), slit-lamp examination, fundus examination, visual fields determined using kinetic perimetry (Goldmann perimeter [GP]; Haag Streit, Bern, Switzerland) and electroretinography (ERG) findings. Characteristic findings for diagnosis of RP include progressive visual field loss from peripheral, night blindness, abnormal color vision, fundus degeneration represented by bone spicule pigmentations and attenuation of retinal vessels, and the more or equally decreased rod responses compared with cone responses of ERG [1,22].

DNA preparation and exome sequencing analysis

We obtained venous blood samples from all participants and genomic DNA was extracted. Whole exome sequencing was performed for 30 arRP/spRP patients using a method previously described [23]. Briefly, construction of paired-end sequence libraries and exome capture were performed by using the Agilent Bravo automated liquid-handling platform with SureSelect XT Human All Exon kit V4+ UTRs kit (Agilent Technologies, Santa Clara, CA). Enriched libraries were sequenced by using an Illumina HiSeq2000 sequencer. Reads were mapped to the reference human genome (1000 genomes phase 2 reference, hs37d5) with Burrows–Wheeler Aligner software version 0.6.2 [24]. Duplicated reads were then removed by Picard Mark Duplicates module version 1.62, and mapped reads around insertion/deletion polymorphisms were realigned by using the Genome Analysis Toolkit (GATK) version 2.1–13 [25]. Base-quality scores were recalibrated by using GATK. To extract potentially RP-causing variants, we focused only on variants that could change the amino acid sequence, such as non-synonymous variants, splice acceptor and donor site variants, and insertion/deletion polymorphisms. The identified variants were filtered by a frequency of less than 1% in the 1000 Genomes project (http://www.1000genomes.org) and the Human Genetic Variation Browser (http://www.genome.med.kyoto-u.ac.jp/SnpDB/about.html). The remained variants were further screened within 212 genes registered as retinal disease-causing genes in the RetNet database updated on March 10, 2014. All remained variants of 30 arRP/spRP patients were summarized in Table S1 in File S1. Selection of disease-causing mutations was restricted to three genetic criteria: first, homozygosity or compound heterozygosity of known arRP-causing mutations; second, compound heterozygosity

Table 2. Identification of patients with *CNGA1* sequence mutations and variants in this study.

Family ID	Exon	Nucleotide Change	Amino Acid Change	State	Frequency*	Polyphen-2 (score)	SIFT (score)	SNP ID	Reference	Pathogenicity
RP#002	5	c.191delG	p.G64Vfs29X	Homo	2				HGVB	Disease-causing
RP#019	6	c.265delC	p.L89FfsX4	Hetero	2				Chen et al. 2013	Disease-causing
	11	c.1429delG	p.V477YfsX17	Hetero	0				This study	
RP#021	5	c.191delG	p.G64Vfs29X	Homo	2				HGVB	Disease-causing
RP#029	6	c.265delC	p.L89FfsX4	Homo	2				Chen et al. 2013	Disease-causing
RP#040	11	cG1271A	p.R424Q	Hetero	7	Benign (0.266)	Damaging (0)	rs192912733	Jin et al. 2008	Not disease-causing
RP#063	11	cG2042C	p.G681A	Hetero	1	Benign (0.001)	Tolerated (0.36)		HGVB	Not disease-causing
RP#087	11	cG860A	p.R287K	Hetero	5	Benign (0.101)	Tolerated (0.32)		HGVB	Not disease-causing
RP#094	6	c.265delC	p.L89FfsX4	Homo	2				Chen et al. 2013	Disease-causing

Polyphen-2 (http://genetics.bwh.harvard.edu/pph2/); SIFT (http://sift.jcvi.org); HGVB = Human Genetic Variation Browser (http://www.genome.med.kyoto-u.ac.jp/SnpDB/about.html); Frequency* show the number of mutations or variants found in 1150 alleles of 575 controls.

doi:10.1371/journal.pone.0108721.t002

of known and predicted arRP-causing mutations; and third, homozygosity or compound heterozygosity of predicted arRP-causing mutations. Mutations were defined as disease causing only if these criteria were fulfilled. Mutations causing exon truncation through frameshift, splicing and termination were considered to be more severe than missense mutations with unknown pathogenic relevance. In addition, to investigate the potential disease-causing variants, we added three genetic criteria: first, compound heterozygosity of known arRP-causing mutation and missense potential arRP-causing variant; second, compound heterozygosity of predicted arRP-causing mutation and potential arRP-causing variant; and third, homozygosity or compound heterozygosity of potential arRP-causing variants.

Direct sequencing of the *CNGA1* gene

The *CNGA1* mutations identified by whole exome sequencing were further confirmed by direct sequencing. An additional 69 arRP/spRP patients were analyzed by direct sequencing for all coding exons (4 to 11) of *CNGA1*. The targeted exons (4 to 11) of the *CNGA1* gene were amplified by PCR using the primer pairs given in Table S2 in File S1. The PCR products were purified using Agencourt APMure XP (Beckman Coulter, Brea, CA) and used as a template for sequencing. Both DNA strands were sequenced by an automated sequencer (3730*xl* DNA Analyzer; Life Technologies Corporation, Carlsbad, CA) using the BigDye Terminator kit V3.1 (Life Technologies Corporation).

Assessment of found mutations or variants in this study

Novel mutations and variants were defined as those not present in the literature, dbSNP database (http://www.ncbi.nlm.nih.gov/SNP/), Human Genetic Variation Browser, 1000 Genome project database or the Human Gene Mutation Database (http://www.hgmd.cf.ac.uk). In addition, the frequency of identified mutations or variants in this study was investigated using in-house exome sequencing data from 575 unaffected Japanese controls at Yokohama City University. Segregation was confirmed for both the arRP-causing mutations and potential arRP-causing variants by direct sequencing when parent samples were available.

Results

Whole exome sequencing analysis and identification of frequent arRP gene mutations

To identify frequent arRP-causing genes, we performed whole exome sequencing in non-syndromic 30 arRP/spRP patients. We focused on 212 retinal disease-causing genes registered in RetNet database updated on March 10, 2014. The average of mean depth for all 30 samples reached 71.11±7.68-fold and the average of coverage at 4- and 12-fold for all 30 samples reached 98.1% and 92.5% respectively. The analysis of arRP-causing mutations and potential arRP-causing variants was conducted according to the criteria described in Materials and Methods. Segregation of identified arRP-causing mutations and potential arRP-causing variants were conducted in five families: RP#002, RP#004, RP#011, RP#016 and RP#019. Although the results of segregation in RP#002, RP#004, RP#016 and RP#019 matched the inheritance pattern, two *USH2A* variants in RP#011 (Table S1 in File S1) did not match the inheritance pattern because the father of RP#011 carried two identical *USH2A* variants. Therefore, we concluded that the two *USH2A* variants in RP#011 were not arRP-causing. Consequently, the exome analysis identified eight arRP-causing mutations including three novel mutations and five known mutations in eight arRP/spRP patients [6,16,26,27] and identified potential arRP-causing

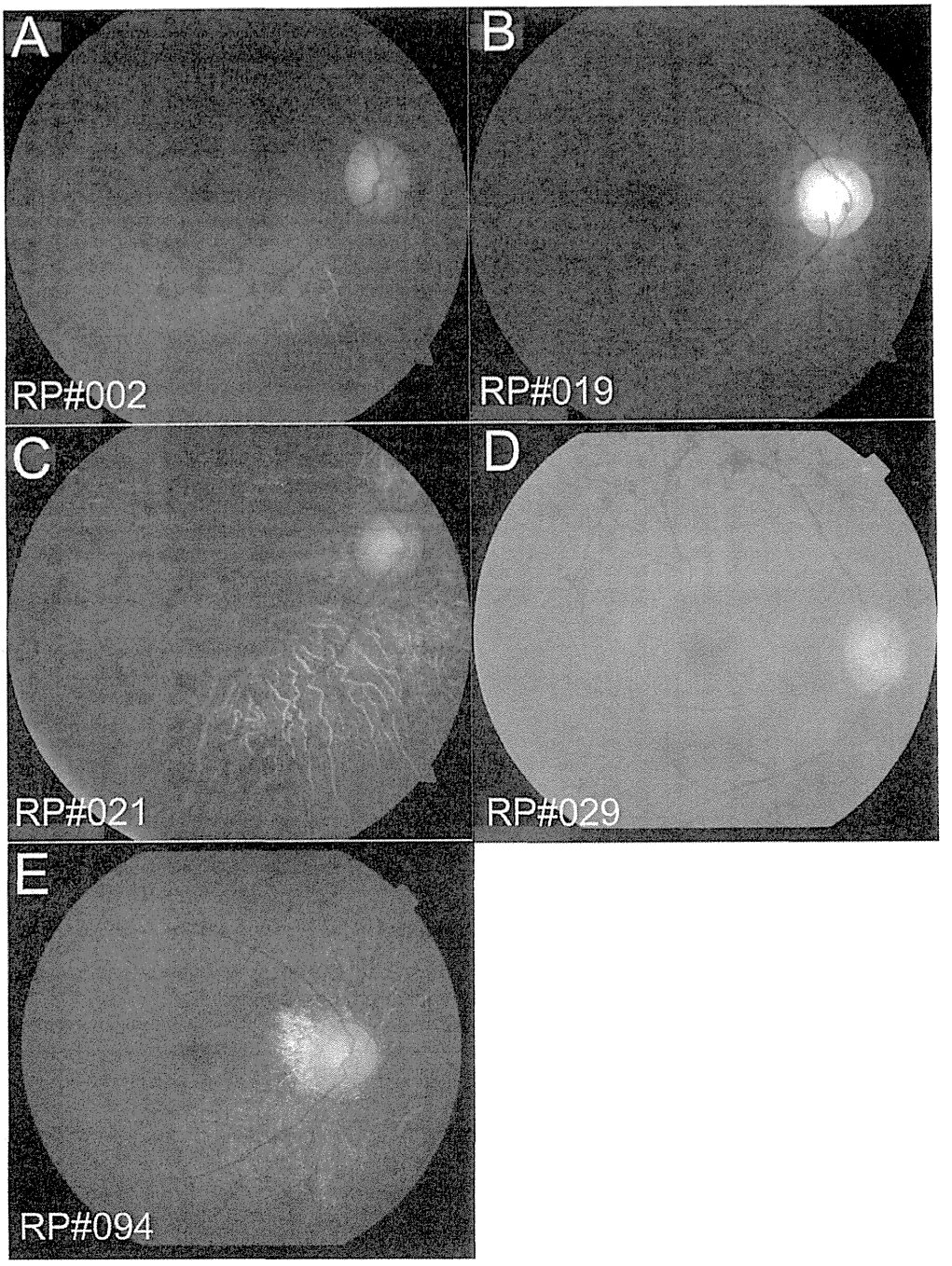

Figure 3. Fundus photographs of the patients with heterozygous or homozygous *CNGA1* mutations. Funduscopy indicates retinal degeneration with pigmentation and attenuation of retinal vessels in all patients. Macular edema does not existed in any patient, although retinal degeneration in the macular region is observed in RP#002, RP#021 and RP#094 (A, C and E).
doi:10.1371/journal.pone.0108721.g003

variants including six novel variants and five known variants in five arRP/spRP patients (Table 1). The arRP-causing mutations were found in *CNGA1* (four patients), *EYS* (three patients) and S-antigen retina and pineal gland (*SAG*) (one patient). Potential arRP-casing variants were found in *USH2A* (two patients), *EYS* (one patient), tubby like protein 1 (*TULP1*) (one patient) and chromosome 2 open reading frame 71 (*C2orf71*) (one patient). Among these genes, the most frequent arRP-causing gene was

Table 3. Ophthalmic findings in five patients with retinitis pigmentosa with compound heterozygous or homozygous *CNGA1* mutations.

Patient	Diagnosed Age, Examined Age, Sex	Onset of night blindness	BCVA		ERG	Visual field	Mutations
			Right	Left			
RP#002	42, 51, M	Childhood	0.5	0.7	Non-recordable	Severely constricted	c.191delG/c.191delG
RP#019	26, 35, F	Childhood	1.0	1.0	Non-recordable	Ring scotoma	c.265delC/c.1429delG
RP#021	60, 65, M	Childhood	0.2	0.1	Non-recordable	Severely constricted	c.191delG/c.191delG
RP#029	25, 51, F	Childhood	1.0	1.0	Non-recordable	Severely constricted	c.265delC/c.265delC
RP#094	16, 46, M	Childhood	0.4	0.3	Non-recordable	Severely constricted	c.265delC/c.265delC

BCVA = decimal corrective visual acuity; ERG = electroretinography; M = male; F = female.

doi:10.1371/journal.pone.0108721.t003

CNGA1. In particular, pedigree RP#002 with a homozygous c.191delG (p.G64VfsX29) mutation, RP#019 with compound heterozygous c.265delC (p.L89FfsX4) and c.1429delG (p.V477YfsX17) mutations, RP#021 with a homozygous c.191delG mutation and RP#029 with a homozygous c.265delC mutation were identified. Further direct sequencing confirmed that the parents in pedigree RP#019 had c.265delC or c.1429delG respectively. The *CNGA1* sequence was compared with the NCBI reference sequence for the *CNGA1* transcript (GenBank ID; NM_000087.3).

Screening of all *CNGA1* exons in 69 additional arRP/spRP Japanese patients

Direct sequencing of the coding region of the *CNGA1* gene in 69 arRP/spRP patients identified homozygous c.265delC mutation in pedigree RP#094 and three heterozygous variants c.G860A (p.R287K), c.G1271A (p.R424Q) and c.G2042C (p.G681A) in pedigrees RP#040, RP#063 and RP#087 respectively. All pedigrees identified to have arRP-causing mutations or potential arRP-causing variants are shown in Figure 1.

Identified *CNGA1* mutations and variants

Among the three arRP-causing mutations and three variants found in this study, two (c.265delC and c.G1271A) were previously reported as arRP-causing or potential arRP-causing [11,26] and four were not reported as arRP-causing or potential arRP-causing (c.191delG, c.265delC, c.G860A and c.G2042C). The polyphen-2 program predicted that all three missense variants in p.R287K (c.G860A), p.R424Q (c.G1271A) and p.G681A (c.G2042C) were benign. In contrast, the SIFT program predicted that p.R424Q (c.G1271A) potentially could cause severe damage to the protein, whereas p.G681A (c.G2042C) and p.R287K (c.G860A) potentially could cause mild damage. All identified mutations and variants in *CNGA1* gene are summarized in Table 2 and sequence data are given in Figure 2.

Haplotype analysis

The haplotypes of *CNGA1* and the surrounding sequences were determined for four arRP patients, RP#002, RP#019, RP#021 and RP#029. Single-nucleotide polymorphisms (SNPs) with a frequency higher than 5% (1000 Genomes project database) were determined within 1 kb upstream and downstream of *CNGA1* (chromosome 4, positions 47,937,994–48,014,961) as shown in Table S3 in File S1. The haplotype analysis determined an identical haplotype for four alleles in patients RP#002 and RP#021 suggesting a common ancestor for the c.191delG mutation. Moreover, identical haplotypes for one allele in patient RP#019 and for both alleles in patient RP#029 were detected suggesting a common ancestor for the c.265delC mutation.

Clinical features of *CNGA1* mutations

To characterize the clinical features of patients with *CNGA1* mutations, we additionally investigated the clinical data of five patients with compound heterozygous or homozygous *CNGA1* mutations (Table 3). All five patients reported that they noticed night blindness from childhood. Funduscopy showed retinal degeneration with pigmentation and attenuation of retinal vessels in all patients (Fig. 3). Macular edema was not observed in any patients, although retinal degeneration in macular regions was detected in RP#002, RP#021 and RP#094 (Fig. 3A, 3C and 3E). The BCVA of RP#019 and RP#029 remained at 1.0, whereas that of RP#002, RP#021 and RP#094 was reduced. ERG showed no recordable pattern in four patients and could not

be conducted in one patient. The GP of RP#022 showed ring scotoma with a preserved peripheral visual field, whereas that of another four patients was severely constricted.

Discussion

Mutations in the *CNGA1* gene were identified for the first time in a Japanese population with a high frequency of 5.1% for homozygous or compound heterozygous mutations. The exome analysis of arRP/spRP patients revealed that 43.3% carried arRP-causing mutations or potential arRP-causing variants in *CNGA1* (13.3%), *EYS* (13.3%), *USH2A* (6.7%), *C2orf71* (3.3%), *SAG* (3.3%) and *TULP1* (3.3%). Although the prevalence of other five gene mutations was consistent with that in previous studies [1,4–8,28–30], the prevalence of *CNGA1* was clearly higher than in population of European descent [31,32]. We screened for mutation in all the coding exons of *CNGA1* in an additional 69 arRP/spRP Japanese patients to further investigate the prevalence of *CNGA1* mutations in the Japanese population. We identified an arRP-causing homozygous *CNGA1* mutation in one patient. Consequently, three *CNGA1* frameshift mutations (c.191delG, c.265delC and c.1429delG) were identified as arRP-causing mutations in five patients (Table 2).

Rod cyclic nucleotide-gated ion channels contain CNGA1 and CNGB1 protein at a ratio of 3 CNGA1:1 CNGB1 [33]. Each molecule of CNGA1 protein has at least three functional domains as described in the UniProtKB (acc. # P29973, http://www.uniprot.org, Cross-References, ProteinModelPortal); these domains function as a cation-transporter domain (residues 202–396, the Pfam ion_trans motif, http://pfam.sanger.ac.uk), cGMP-binding domain (residues 404–596, SWISSMODEL structure based on the PDB file: 4hbn_A, http://www.rcsb.org/pdb/home/home.do) and carboxy-terminal leucine zipper (CLZ) domain (residues 623–690, experimental structure based on the PDB file:3swf). The p.G64VfsX29 (c.191delG) and p.L89FfsX4 (c.265delC) protein had no transmembrane lesions, and most of the protein structure including all three functional domains was abolished. In contrast, the p.V477YfsX17 (c.1429delG) mutant protein had the correct structure up to 5th transmembrane domain helix, but lacked the 6th transmembrane domain helix, the cGMP-binding site, and the coiled-coil CLZ domain. The cGMP-binding site is important for the function of CNGA1 as a cation channel. Loss of the cGMP-binding site is likely to influence the final stage of the photo transduction pathway [31]. In addition, the absence of the coiled-coil CLZ domain completely disrupts the 3:1 stoichiometry in CNG channels [33]. Although the p.V477YfsX17 (c.1429delG) mutant may retain part of its structure, the protein function is predicted to be completely lost.

We additionally identified the heterozygous *CNGA1* missense variants c.G860A (p.R287K), c.G1271A (p.R424Q) and c.G2042C (p.G681A) (Table 2). Heterozygous c.G1271A variant has been previously reported [11]. Based on the mild score given by the polyphen-2 program and the severe score given by the SIFT program, we also predicted that this variant is potentially disease causing. In contrast, the two novel missense variants c.G860A and c.G2042C were predicted to cause mild damage by both the polyphen-2 and SIFT programs suggesting that it is non-pathogenic. Overall, all three missense *CNGA1* variants (c.G860A, c.G1271A and c.G2042C) were found in only one allele of *CNGA1*. We conclude that these three *CNGA1* variants were not disease causing in nature, at least from the phenotypic observation.

The clinical course of the five patients with compound heterozygous or homozygous *CNGA1* mutations included night blindness from childhood, visual field loss in middle age, non-recordable ERG and characteristic retinal degeneration pattern of RP, which were consistent with previously reported phenotypes of *CNGA1* mutations [32,34]. Retinal degeneration in the macular region and severely decreased BCVA occurred in 3/5 patients suggesting that the advanced stage of *CNGA1* mutations included degeneration of the entire retina with both rod and cone photoreceptors. Although the genotype-phenotype correlation for *CNGA1* mutations was not clear in this study, all five patients with *CNGA1* mutations showed typical phenotypes of RP.

Previous reports have shown a strong association of *CNGA1* with arRP [11,26,31,32,34,35]. Dryja et al. estimated the prevalence of *CNGA1* mutations in arRP patients to be between 1.7 and 2.3% (3 or 4 of 173 patients) [31]. The prevalence of *CNGA1* mutations in a Spanish arRP population was 2.1% (1 of 46 patients) [32], whereas that in a Chinese population with hereditary retinal dystrophy was 4.0% (1 of 25 patients) [26]. The average prevalence of *CNGA1* mutations in arRP/spRP patients was 7.6% (1 of 13 patients) [26]. These findings suggest that the prevalence of *CNGA1* mutations is higher in Asian population than in populations of European descent. The prevalence of *CNGA1* mutations in Chinese populations requires further study because only one Chinese patient has been reported to have a homozygous mutation in this gene [26]. Jin et al. investigated *CNGA1* exons 6, 8 and partial 11 in 193 Japanese RP families and found a single heterozygous *CNGA1* variant (c.1271G>A) [11]. In our study, all coding exons of *CNGA1* were screened and the estimate prevalence of *CNGA1* mutations reached at 5.1% (5 of 99 patients) including four homozygous and one compound heterozygous patients. Our findings suggest that the prevalence of *CNGA1* mutations is higher in Asian populations than in European populations. Moreover, c.191delG mutation has only been reported in Human Genetic Variation Browser (the database of genetic variations in Japanese population, http://www.genome.med.kyoto-u.ac.jp/SnpDB/), c.265delC mutation only reported in Chinese population [26] and c.1429delG mutation identified as novel. The *CNGA1* mutations found in this study only overlapped with mutations identified in studies of Asian individuals indicating that the founder is specific to Asian populations. Lastly, the haplotypes for the *CNGA1* mutations found in this study were individually unique (Table S3 in File S1). Further investigation of haplotypes is required to clarify the origin of these *CNGA1* mutations.

Supporting Information

File S1 Supporting Tables. Table S1, All rare variants of 30 arRP/spRP paients of this study, focusing on 212 retinal disease-causing genes registered in the Retinal Information Network (https://sph.uth.edu/retnet/). Table S2, *CNGA1* primers and PCR conditions. Table S3, Haplotype analysis of four retinitis pigmentosa patients with *CNGA1* mutations.
(DOC)

Acknowledgments

We thank the patients and their families for participation in this study. The authors wish to acknowledge RIKEN GeNAS for the sequencing of the exome-enriched libraries using the Illumina HiSeq2000.

Author Contributions

Conceived and designed the experiments: TI SK. Performed the experiments: SK MA YS KY KI MF TH MK SU KT KS KK YT NM. Analyzed the data: SK MA TI. Contributed reagents/materials/analysis tools: HT. Wrote the paper: SK TI.

References

1. Hartong DT, Berson EL, Dryja TP (2006) Retinitis pigmentosa. Lancet 368: 1795–1809.
2. Mansergh FC, Millington-Ward S, Kennan A, Kiang AS, Humphries M, et al. (1999) Retinitis pigmentosa and progressive sensorineural hearing loss caused by a C12258A mutation in the mitochondrial MTTS2 gene. Am J Hum Genet 64: 971–985.
3. Kajiwara K, Berson EL, Dryja TP (1994) Digenic retinitis pigmentosa due to mutations at the unlinked peripherin/*RDS* and *ROM1* loci. Science 264: 1604–1608.
4. Rivolta C, Sweklo EA, Berson EL, Dryja TP (2000) Missense mutation in the *USH2A* gene: association with recessive retinitis pigmentosa without hearing loss. Am J Hum Genet 66: 1975–1978.
5. Abd El-Aziz MM, Barragan I, O'Driscoll CA, Goodstadt L, Prigmore E, et al. (2008) *EYS*, encoding an ortholog of Drosophila spacemaker, is mutated in autosomal recessive retinitis pigmentosa. Nat Genet 40: 1285–1287.
6. Collin RW, Littink KW, Klevering BJ, van den Born LI, Koenekoop RK, et al. (2008) Identification of a 2 Mb human ortholog of Drosophila eyes shut/spacemaker that is mutated in patients with retinitis pigmentosa. Am J Hum Genet 83: 594–603.
7. Abd El-Aziz MM, O'Driscoll CA, Kaye RS, Barragan I, El-Ashry MF, et al. (2010) Identification of novel mutations in the ortholog of Drosophila eyes shut gene (*EYS*) causing autosomal recessive retinitis pigmentosa. Invest Ophthalmol Vis Sci 51: 4266–4272.
8. Audo I, Sahel JA, Mohand-Said S, Lancelot ME, Antonio A, et al. (2010) *EYS* is a major gene for rod-cone dystrophies in France. Hum Mutat 31: E1406–1435.
9. Bandah-Rozenfeld D, Littink KW, Ben-Yosef T, Strom TM, Chowers I, et al. (2010) Novel null mutations in the *EYS* gene are a frequent cause of autosomal recessive retinitis pigmentosa in the Israeli population. Invest Ophthalmol Vis Sci 51: 4387–4394.
10. Klevering BJ, Yzer S, Rohrschneider K, Zonneveld M, Allikmets R, et al. (2004) Microarray-based mutation analysis of the *ABCA4* (*ABCR*) gene in autosomal recessive cone-rod dystrophy and retinitis pigmentosa. Eur J Hum Genet 12: 1024–1032.
11. Jin ZB, Mandai M, Yokota T, Higuchi K, Ohmori K, et al. (2008) Identifying pathogenic genetic background of simplex or multiplex retinitis pigmentosa patients: a large scale mutation screening study. J Med Genet 45: 465–472.
12. Fujiki K, Hotta Y, Hayakawa M, Sakuma H, Shiono T, et al. (1992) Point mutations of rhodopsin gene found in Japanese families with autosomal dominant retinitis pigmentosa (ADRP). Jpn J Hum Genet 37: 125–132.
13. Saga M, Mashima Y, Akeo K, Oguchi Y, Kudoh J, et al. (1994) Autosomal dominant retinitis pigmentosa. A mutation in codon 181 (Glu–>Lys) of the rhodopsin gene in a Japanese family. Ophthalmic Genet 15: 61–67.
14. Fujiki K, Hotta Y, Murakami A, Yoshii M, Hayakawa M, et al. (1995) Missense mutation of rhodopsin gene codon 15 found in Japanese autosomal dominant retinitis pigmentosa. Jpn J Hum Genet 40: 271–277.
15. Hosono K, Ishigami C, Takahashi M, Park DH, Hirami Y, et al. (2012) Two novel mutations in the *EYS* gene are possible major causes of autosomal recessive retinitis pigmentosa in the Japanese population. PLoS One 7: e31036.
16. Iwanami M, Oshikawa M, Nishida T, Nakadomari S, Kato S (2012) High prevalence of mutations in the *EYS* gene in Japanese patients with autosomal recessive retinitis pigmentosa. Invest Ophthalmol Vis Sci 53: 1033–1040.
17. Shendure J, Ji H (2008) Next-generation DNA sequencing. Nat Biotechnol 26: 1135–1145.
18. Mardis ER (2008) The impact of next-generation sequencing technology on genetics. Trends Genet 24: 133–141.
19. Mardis ER (2008) Next-generation DNA sequencing methods. Annu Rev Genomics Hum Genet 9: 387–402.
20. Ansorge WJ (2009) Next-generation DNA sequencing techniques. N Biotechnol 25: 195–203.
21. Shanks ME, Downes SM, Copley RR, Lise S, Broxholme J, et al. (2013) Next-generation sequencing (NGS) as a diagnostic tool for retinal degeneration reveals a much higher detection rate in early-onset disease. Eur J Hum Genet 21: 274–280.
22. Berson EL (1993) Retinitis pigmentosa. The Friedenwald Lecture. Invest Ophthalmol Vis Sci 34: 1659–1676.
23. Katagiri S, Yoshitake K, Akahori M, Hayashi T, Furuno M, et al. (2013) Whole-exome sequencing identifies a novel *ALMS1* mutation (p.Q2051X) in two Japanese brothers with Alström syndrome. Molecular Vision 19: 2393–2406.
24. Li H, Durbin R (2009) Fast and accurate short read alignment with Burrows-Wheeler transform. Bioinformatics 25: 1754–1760.
25. McKenna A, Hanna M, Banks E, Sivachenko A, Cibulskis K, et al. (2010) The Genome Analysis Toolkit: a MapReduce framework for analyzing next-generation DNA sequencing data. Genome Res 20: 1297–1303.
26. Chen X, Zhao K, Sheng X, Li Y, Gao X, et al. (2013) Targeted sequencing of 179 genes associated with hereditary retinal dystrophies and 10 candidate genes identifies novel and known mutations in patients with various retinal diseases. Invest Ophthalmol Vis Sci 54: 2186–2197.
27. Fuchs S, Nakazawa M, Maw M, Tamai M, Oguchi Y, et al. (1995) A homozygous 1-base pair deletion in the arrestin gene is a frequent cause of Oguchi disease in Japanese. Nat Genet 10: 360–362.
28. Hagstrom SA, North MA, Nishina PL, Berson EL, Dryja TP (1998) Recessive mutations in the gene encoding the tubby-like protein TULP1 in patients with retinitis pigmentosa. Nat Genet 18: 174–176.
29. Nakazawa M, Wada Y, Tamai M (1998) Arrestin gene mutations in autosomal recessive retinitis pigmentosa. Arch Ophthalmol 116: 498–501.
30. Collin RW, Safieh C, Littink KW, Shalev SA, Garzozi HJ, et al. (2010) Mutations in *C2ORF71* cause autosomal-recessive retinitis pigmentosa. Am J Hum Genet 86: 783–788.
31. Dryja TP, Finn JT, Peng YW, McGee TL, Berson EL, et al. (1995) Mutations in the gene encoding the alpha subunit of the rod cGMP-gated channel in autosomal recessive retinitis pigmentosa. Proc Natl Acad Sci U S A 92: 10177–10181.
32. Paloma E, Martinez-Mir A, Garcia-Sandoval B, Ayuso C, Vilageliu L, et al. (2002) Novel homozygous mutation in the alpha subunit of the rod cGMP gated channel (*CNGA1*) in two Spanish sibs affected with autosomal recessive retinitis pigmentosa. J Med Genet 39: E66.
33. Shuart NG, Haitin Y, Camp SS, Black KD, Zagotta WN (2011) Molecular mechanism for 3:1 subunit stoichiometry of rod cyclic nucleotide-gated ion channels. Nat Commun 2: 457.
34. Zhang Q, Zulfiqar F, Riazuddin SA, Xiao X, Ahmad Z, et al. (2004) Autosomal recessive retinitis pigmentosa in a Pakistani family mapped to CNGA1 with identification of a novel mutation. Mol Vis 10: 884–889.
35. Gonzalez-del Pozo M, Borrego S, Barragan I, Pieras JI, Santoyo J, et al. (2011) Mutation screening of multiple genes in Spanish patients with autosomal recessive retinitis pigmentosa by targeted resequencing. PLoS One 6: e27894.

Original Paper

Ophthalmologica

Ophthalmologica 2014;232:118–125
DOI: 10.1159/000361056

Received: August 18, 2013
Accepted after revision: February 28, 2014
Published online: June 24, 2014

Multifocal Electroretinograms in Stargardt's Disease/Fundus Flavimaculatus

Kazuki Kuniyoshi[a, c] Hiroko Terasaki[a, d] Mikki Arai[a, e] Tatsuo Hirose[a, b]

[a]Schepens Eye Research Institute, Harvard Medical School, Boston, Mass., and [b]Boston Eye Group, Brookline, Mass., USA; [c]Department of Ophthalmology, Kinki University Faculty of Medicine, Osaka, [d]Department of Ophthalmology, Nagoya University Graduate School of Medicine, Nagoya, and [e]Arai Eye Clinic, Fukuoka, Japan

Key Words
Stargardt's disease · Fundus flavimaculatus · Electroretinography · Multifocal electroretinography · Macular dystrophy · Macular degeneration · Retinal dystrophy · Retinal degeneration · *ABCA4*

Abstract
Purpose: To determine whether the characteristics of multifocal electroretinograms (mfERGs) were correlated with the ophthalmic appearance of the fundus in patients with Stargardt's disease/fundus flavimaculatus (SFF). ***Methods:*** Full-field ERGs, mfERGs, and general ophthalmic examinations were performed on 49 eyes with SFF. ***Results:*** The SFF patients were divided into four subtypes according to the classification of Noble and Carr [Arch Ophthalmol 1979;97:1281–1285]. The patients with type 1 SFF had severely reduced mfERGs in the macular area and reduced and delayed responses in the mid-periphery. The type 2 SFF patients had reduced but recordable mfERGs from the center of the macula with more depressed responses in the paramacular area, and the type 3 SFF patients had reduced and delayed mfERGs both in the macula and periphery. The patients with type 4 SFF had normal mfERGs in the macular area and delayed responses in all outer zones. ***Conclusions:*** These mfERG findings indicate that each subtype of SFF has unique characteristics corresponding to the abnormal retinal functions.

Introduction

Stargardt's disease was first reported in 1909 as a juvenile-onset, bilateral, hereditary macular dystrophy [1]. In 1962, Franceschetti [2] coined the term 'fundus flavimaculatus' to describe a type of retinal degeneration characterized by diffuse yellowish flecks affecting the posterior and, occasionally, the peripheral fundus. He reported that some cases also had macular degeneration [2, 3]. Stargardt's disease and fundus flavimaculatus usually have an autosomal recessive inheritance pattern [1–16] and rarely an autosomal dominant pattern [17].

In 1967, Klien and Krill [4] proposed a system for classifying the abnormalities seen in Stargardt's disease and fundus flavimaculatus. Since then, these two conditions have been considered to be the same clinical entity, and called 'Stargardt's disease/fundus flavimaculatus' (SFF). Because SFF is a complex retinal dystrophy with wide variations in phenotype, it is generally diagnosed by fundus findings and fluorescein angiograms [5]. Recently, fundus autofluorescence imaging has been reported to be helpful in evaluating the status of the photoreceptors/retinal pigment epithelium in eyes with SFF [10–16]. Foveal sparing, which was observed by ophthalmoscopy and/or fundus autofluorescence imaging, was reported to be present in patients with slowly progressing SFF and relatively good visual acuity [11, 13, 14].

KARGER

E-Mail karger@karger.com
www.karger.com/oph

0030–3755/14/2322–0118$39.50/0

Kazuki Kuniyoshi, MD
Department of Ophthalmology, Kinki University Faculty of Medicine
377-2 Ohno-Higashi
Osaka-Sayama City, Osaka 589-8511 (Japan)
E-Mail kazuki@med.kindai.ac.jp

Table 1. Outline of patient characteristics

Patient No.	Age/sex	BCVA	Fundus		Type	Full-field ERG		mfERG		Choroidal silence in FA
			macular degeneration	flecks		photopic b-wave	scotopic b-wave	P1 average	P1 in zone 1	
1	42/M	20/100 OU	yes	no	1	75%	66%	60%	0%	posterior pole
2	16/F	20/30 OU	yes	no	1	–	–	71%	0%	diffuse
3	7/F	20/200 OD	yes	no	1	66%	100%	74%	0%	–
4	45/F	20/200 OU	yes	no	1	–	–	100%	0%	posterior pole
5	30/M	20/200 OU	yes	paramacular	2	–	–	66%	74%	diffuse
6	25/F	20/200 OU	yes	paramacular	2	100%	86%	75%	0%	posterior pole
7	26/M	20/50 OD	yes	paramacular	2	100%	100%	92%	38%	diffuse
		20/200 OS	yes	paramacular	2	100%	100%	65%	50%	diffuse
8	37/F	20/100 OD	yes	paramacular	2	80%	100%	100%	52%	–
		20/30 OS	yes	paramacular	2	80%	100%	97%	0%	–
9	26/M	20/40 OU	yes	paramacular	2	–	–	100%	75%	diffuse
10	30/F	20/20 OU	yes	paramacular	2	100%	100%	100%	100%	posterior pole
11	43/M	20/400 OU	yes	diffuse	3	30%	60%	16%	0%	diffuse
12	29/F	20/400 OU	yes	diffuse	3	35%	70%	31%	0%	diffuse
13	18/F	20/300 OU	yes	diffuse	3	60%	76%	33%	0%	posterior pole
14	45/M	20/200 OU	yes	diffuse	3	100%	100%	40%	23%	diffuse
15	23/F	CF 8′ OU	yes	diffuse	3	50%	50%	45%	0%	diffuse
16	36/M	20/200 OU	yes	diffuse	3	50%	90%	50%	38%	diffuse
17	67/F	20/400 OU	yes	diffuse	3	104%	103%	58%	24%	diffuse
18	61/F	20/300 OU	yes	diffuse	3	50%	100%	62%	0%	–
19	37/F	20/200 OU	yes	diffuse	3	70%	100%	66%	0%	diffuse
20	48/M	20/200 OU	yes	diffuse	3	–	–	72%	0%	diffuse
21	24/F	20/200 OU	yes	diffuse	3	–	–	91%	40%	–
22	42/F	20/50 OD	yes	diffuse	3	–	–	100%	0%	diffuse
		20/200 OS	yes	diffuse	3	–	–	84%	0%	diffuse
23	32/M	20/20 OU	no	diffuse	4	50%	70%	65%	107%	diffuse
24	55/M	20/25 OS	no	diffuse	4	–	–	66%	80%	diffuse
25	55/F	20/15 OS	no	diffuse	4	–	–	100%	100%	diffuse
26	47/F	20/20 OU	no	diffuse	4	–	–	100%	100%	–

ERG b-wave amplitudes and P1 response density were expressed as percent of the lower/upper limit of age-matched normal values; 100% means within normal values. BCVA = Best-corrected visual acuity; FA = fluorescein angiography; OU/OD/OS = oculus uterque/dexter/sinister; – = no data were obtained; CF = counting fingers.

In 1997, Allikmets et al. [18] identified a mutation in the *ABCR (ABCA4)* gene in patients with Stargardt's macular dystrophy. This report was followed by other studies which showed that *ABCA4* gene mutations can also cause retinitis pigmentosa [19–21] and cone-rod dystrophy [21, 22]. All of these diseases have been grouped into one group called '*ABCA4*-associated retinal diseases' [23]. The purpose of this study was to determine whether the characteristics of multifocal electroretinograms (mfERGs) were different between the four subtypes of SFF.

Subjects and Methods

The patients were classified into four types according to the classification of Noble and Carr [6]. Type 1 eyes had macular degeneration without flecks (7 eyes, 4 patients), type 2 eyes had macular degeneration with parafoveal flecks (12 eyes, 6 patients), type 3 eyes had macular degeneration with diffuse flecks (24 eyes, 12 patients), and type 4 eyes had diffuse flecks with no macular degeneration (6 eyes, 4 patients; table 1; fig. 1). All patients had the same type of disease bilaterally.

We recorded mfERGs from 49 eyes of 26 patients with SFF disease and from 17 age-matched normal control subjects. The mean age ± standard deviation of the 26 patients with SFF was 36 ± 14

Ophthalmologica 2014;232:118–125
DOI: 10.1159/000361056

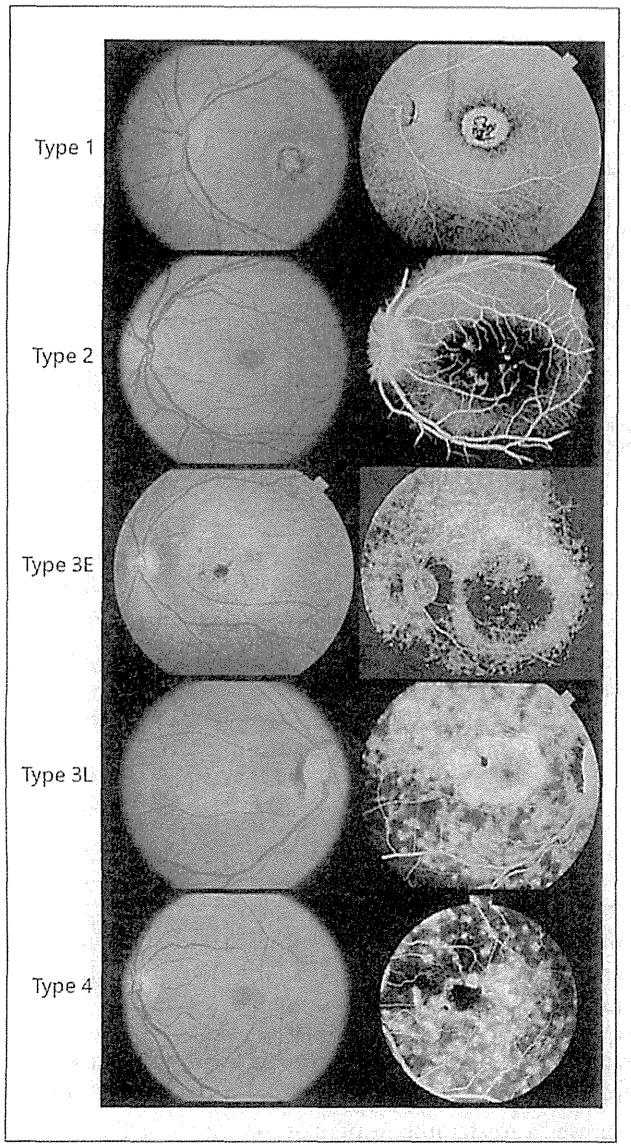

Fig. 1. Fundus photographs (left) and fundus fluorescein angiograms (right) of eyes with type 1 (patient 1), type 2 (patient 10), type 3E (patient 11), type 3L (patient 19), and type 4 SFF (patient 25). Type 3 was divided into two subtypes: early onset (3E) and late onset (3L).

years, with a range of 7–67 years. The mean age of the normal subjects was 37 ± 17 years, with a range of 22–66 years.

The procedures used in this study conformed to the tenets of the Declaration of Helsinki. Before the mfERG recordings, the benefits and risks of the procedures were explained to the older patients, the parents or guardians of minor patients, and the normal subjects. All participants signed an informed consent form.

After dilating the pupil, mfERGs were recorded using a Burian-Allen bipolar contact lens electrode with the Veris II mfERG system (Tomey, Nagoya, Japan). The stimulus matrix had 61 elements arranged over a hexagonal 40° × 50° field. A small red dot or cross was displayed at the center of the CRT monitor as the point of fixation for the subject. For patients with poor vision, a larger cross was used for visual fixation, and the eye fixation was monitored with an infrared camera during the examination. The recordings which had high noise levels caused by eye movements or blinking were discarded, and the mfERGs were recorded again.

The 61 mfERGs were divided into five concentric groups (fig. 2, left). The responses were averaged for each zone, and the distributions of the response densities and implicit times were calculated for each zone. A three-dimensional (3D) map of the response densities was also made, using the methods of Sutter and Tran [24]. Static analysis was not performed, because of the small number of cases especially of type 1 and type 4 SFF. General ophthalmic examinations including ophthalmoscopy, measurements of visual acuity, full-field ERGs, fundus photography, and fluorescein angiography were performed prior to the mfERG recordings.

Results

The demographics of the patients as well as the results of fundus photography and fluorescein angiography are shown in table 1 and figure 1. Typical mfERG recordings and a 3D representation of the response density of each type are shown in figure 3. The values for response density and implicit time are shown in figure 4.

The mfERGs recorded from the normal subjects had two major components: a cornea-negative wave followed by a cornea-positive wave (N1 and P1 [25]; fig. 2, right). The highest density of P1 was in zone 1, and the density decreased rapidly in zones 2–5, as shown by the thick lines in the left column of figure 4. The implicit time of P1 was longest in zone 1 and became shorter in zones 2 and 3 (thick lines; fig. 4, right). mfERGs were recorded from both eyes of all but 3 patients; patient 3 did not have mfERGs recorded from the second eye because of her young age, and patients 25 and 26 had had penetrating ocular trauma in their untested eyes.

All eyes with type 1 SFF (n = 7) had reduced full-field ERG photopic b-waves and 2 of 3 eyes tested had reduced scotopic b-waves (table 1). The mfERG response in zone 1 was at the noise level, and the responses in zone 2 were considerably reduced (table 1; fig. 3, 4). In the periphery (zone 5), all eyes had P1 with a normal response density (fig. 4).

In type 2 SFF (n = 12), 6 of 8 eyes had normal full-field ERG photopic b-waves and normal scotopic b-waves. The mfERGs of 9 of the 12 eyes were reduced in zone 1, and all eyes had reduced response densities in zone 2

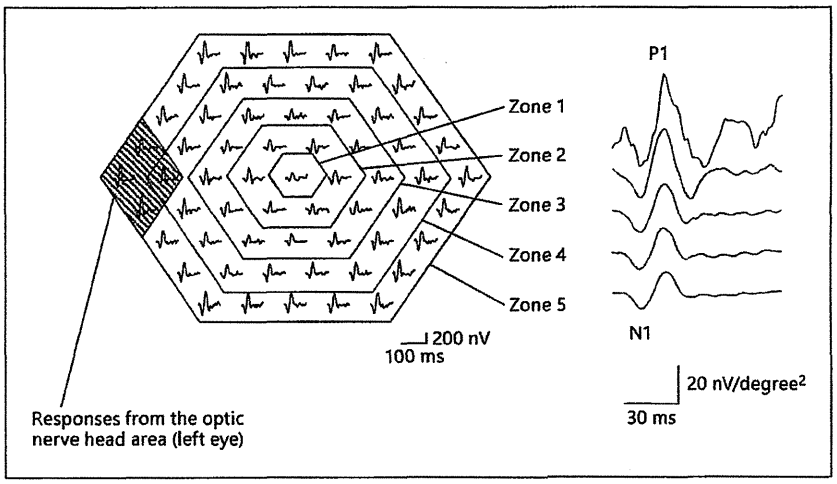

Fig. 2. Schematic diagram of the mfERG responses from each of the 61 areas (left) and averaged responses from each zone of a normal eye (right).

(fig. 4). This resulted in a ring-shaped valley surrounding the central peak in the 3D map (fig. 3). Both eyes of patient 10 showed foveal sparing at a vision of 20/20 with normal mfERGs for zone 1. The response densities of the mfERGs in zone 5 were normal, but the implicit times were delayed in zones 4 and 5 in 7 and 3 eyes of the 12 eyes, respectively (fig. 4).

In type 3 SFF, 12 of 18 eyes had reduced (≤60%) full-field photopic b-waves and 4 of 18 eyes had reduced (≤60%) scotopic b-waves (table 1). The mfERGs were nonrecordable or markedly reduced in all eyes in zone 1, and they were also reduced in zones 2 and 3 in all eyes except the right eye of patient 22, which had a reduced mfERG but within normal limits (table 1; fig. 4). The responses in zones 4 and 5 were reduced in most patients, but the deviation from low normal was not large. The implicit time was delayed in 20 of the 24 eyes in zones 2–5 (fig. 4).

In type 4 SFF, 2 of the 6 eyes had reduced full-field photopic and scotopic b-waves. The response density of the mfERGs was normal in 5 eyes in zone 1, in 4 eyes in zone 2, and in 3 eyes in zones 3–5 (table 1; fig. 4). The implicit time was delayed in all eyes in zones 2–4, and in 4 of the 6 eyes in zone 5 (fig. 4).

Discussion

Our results show that each type of SFF has characteristic mfERG findings which have not been reported so far. A few investigators have examined mfERGs of patients with SFF [11, 26, 27], and Maia-Lopes et al. [27] reported a reduction or nonrecordable responses from the macular area in their patients and their relatives who were carriers and had few visible macular abnormalities.

From our mfERG results, type 1 and type 3 SFF have similar electrophysiological characteristics in two ways. The reduction in response density in zone 2 in eyes with type 1 SFF (fig. 4) indicates that the retinal impairment spreads to the paramacular area where the degeneration is not visible yet, and in eyes with type 3 SFF, the reduction and the delay of the mfERGs in all zones suggest that the impairment of the retina has spread from the macular area to the mid-periphery. These results indicate that the impairment of the cones in type 1 and type 3 SFF has spread beyond the ophthalmoscopically visible retinal degeneration. Another electrophysiological similarity between type 1 and type 3 SFF was that the full-field ERGs showed a greater impairment of cone function than of rod function (table 1), as previously reported [7, 8, 28]. The averaged response density of P1 of the mfERGs was decreased in 28 of the 31 eyes with type 1 or type 3 SFF (table 1), which also indicates an impairment of the cone system in these patients.

In the advanced stage of type 3 SFF, the mfERGs were diffusely reduced and resembled the findings in advanced cone-rod dystrophy or retinitis pigmentosa. This is consistent with previous reports on SFF with an early onset and a poor prognosis [7, 8], or on SFF with a rapid decline of vision [29], and genetic studies have shown that mutations of the *ABCA4* gene can cause not only Stargardt's disease [18] but also retinitis pigmentosa [19–21] and cone-rod dystrophy [21, 22].